# Through-the-jacket inscription of fiber Bragg gratings using femtosecond infrared radiation for sensor applications

Stephen J. Mihailov, Dan Grobnic, Christopher W. Smelser and Robert B. Walker
Communications Research Centre Canada, 3701 Carling Avenue, Ottawa, ON Canada K2H 8S2

## ABSTRACT

Silica-based fiber Bragg gratings (FBG) sensors are versatile devices that are typically fabricated using UV laser exposure. As most standard optical fiber polymer coatings are highly absorbing in the UV, grating inscription typically requires the removal and reapplication of the protective coating by either chemical or mechanical means. Optical fiber stripping and recoating are time-consuming processes that can seriously degrade the mechanical integrity of the fiber. For high temperature sensor applications (> 200 °C), the optical fiber is coated in polyimide which is resistant to chemical attack. Invasive and hazardous techniques for its removal are required such as hot sulphuric acid stripping. In this paper, results of FBG inscription directly through the polymer coating of standard optical fiber with a femtosecond infrared laser and a phase mask are reviewed. Significant grating reflectivities are achieved along with improved mechanical reliability and performance at elevated temperatures. The only example of direct FBG inscription through polyimide coatings for high temperature stable grating sensors will also be presented.

**Keywords:** Fiber Bragg gratings, photosensitivity, Fiber optics sensors, Ultrafast processes in Fibers

## 1. INTRODUCTION

For more than a decade, the fiber Bragg grating (FBG) has proven itself to be a cost effective and versatile component in optical fiber based sensing systems [1]. Variations in the FBG spectral response can be correlated to the strain and temperature that are applied directly to the grating structure making the FBG an effective sensing element. A practical and commercial incentive for the development of mechanically strong and high-temperature resistant FBGs is the present need for temperature and strain sensors within the automotive, aerospace, electrical power, industrial process as well as the oil & gas industries that are capable of measuring static and dynamic stresses under harsh environments and at elevated temperatures (>200 °C). Typical applications are strain monitoring in manifolds for gas and diesel engines; strains in jet turbine blades; power plant pipeline and furnace stress measurement; oil & gas reservoir monitoring; stresses and crack monitoring on airplane wings, rocket boosters and fuselages; and many others. At these elevated temperatures, conventional foil strain gauges cannot operate. As an alternative, engineers have resorted to the use of free-filament and weldable resistive gauges, devices which themselves present performance limitations due to thermal errors, large zero drifts, non repeatable readings, difficult signal conditioning, and susceptibility to moisture and electromagnetic interference (EMI). FBGs, in contrast, offer a number of inherent advantages such as the capability to perform quasi-distributed measurements along the length of a single optical fiber, wavelength encoded output, immunity from EMI and a large temperature range of operation.

Typically, FBG inscription is performed using high power ultraviolet laser sources [2]. The protective polymer coatings of standard optical fibers are highly absorbing at the UV irradiating wavelengths needed to create the photo-induced index changes that are required for grating formation. In order to write the FBG, the polymer coating is typically removed from the fiber by either mechanical or chemical means. From a manufacturing and device reliability point of view, coating removal and replacement are undesirable processes as they are time-consuming and often reduce the mechanical integrity of the fiber. For some high temperature FBG applications, fibers have polymer coatings such as polyimide that are thermally stable up to 400 °C. Polyimide is resistant to chemical attack and requires invasive and hazardous techniques for its removal such as hot sulphuric acid stripping. The fiber is then recoated subsequent to the FBG inscription [3]. Polyimide coating removal and replacement are undesirable processes from a manufacturing viewpoint as they are hazardous, time-consuming and threaten the mechanical integrity of the fiber. Therefore, development of a through-the-coating grating writing process not only can lead to a high-temperature resistant FBG but, more importantly, make for a mechanically strong device thus helping to ensure long-term durability and reliability. Such reliability is particularly critical in FBG sensing arrays.

Fiber Optic Sensors and Applications VI, edited by Eric Udd, Henry H. Du, Anbo Wang, Proc. of SPIE Vol. 7316, 73160B

Several groups have investigated UV-laser FBG inscription through the protective polymer coating over the last decade. Using the near-UV 334 nm line from an $Ar^+$ laser, weak gratings were inscribed through the standard coating of high Ge-doped fibers producing an index modulation $\Delta n = 5 \times 10^{-5}$ [4]. Specialized UV-transmissive polymer coatings have been used with standard UV sources to produce stronger grating structures [5-7]. Grating inscription in a boron co-doped UV photosensitive fiber with a standard silicone rubber coating at 244 nm was reported [8], however silicone rubber still has significant absorption at standard UV grating inscription wavelengths and is difficult to remove from fibers when preparing their ends for integration into network systems. This difficulty in handling is the major reason why silicone rubber coatings are no longer used on standard fibers. Although FBGs have been inscribed without coating removal by using these special coatings with higher transparency to UV radiation, [5,6,8] these coatings are typically not stable at higher temperatures. Recently the inscription of an FBG array through a specialty UV-transmissive coating was reported where the coating was thermally stable up to 220 °C [7]. Although an improvement, the coating is still not as thermally stable as polyimide. The use of non-standard coatings and fibers is undesirable from an industrial FBG manufacturing perspective as custom fiber designs and coatings are inherently more expensive.

Recently, FBG inscription through the polymer coatings of standard optical fibers were reported using femtosecond (fs) infrared (IR) radiation with either the point-by-point method [9] or a phase mask [10-12]. In ref. [9], the tight focusing geometry of the point-by-point method resulted in a large difference in beam intensities at the fiber coating and core, thus making it possible to induce a substantial index modulation ($\Delta n$) in the core ($3 \times 10^{-4}$) without damaging the coating. For mass production, FBG fabrication by the point-by-point technique is less desirable when compared to the phase mask technique as FBGs defined by a phase mask are more easily reproduced. Furthermore, the $\Delta n$ of the point-by-point technique results from a plasma formation that produces microvoids [13]. Although thermally stable up to the glass transition temperature of the fiber, such a damage type structure reduces the fiber strength.

In this review paper we will be summarizing the work performed on grating inscription through the polymer coatings of various fibers with the femtosecond IR laser and phase mask technique.

## 2. EXPERIMENT

Bragg gratings were fabricated in commercially available standard single mode Ge-doped optical fibers, specifically low Ge concentration acylate coated SMF-28 fiber from *Corning*, and various high numerical aperture (NA), high Ge-content acylate and polyimde coated fibers from various manufacturers. Table I summarizes the properties of all the fibers that were evaluated.

Table 1. Fibers Evaluated

| Manufacturer | Name | Mode Field Diameter (μm) | $\lambda_{cutoff}$ (nm) | NA | Core diameter (μm) | Fiber coating | Coating thickness (μm) |
|---|---|---|---|---|---|---|---|
| *Corning* | SMF-28 | 10.4 | 1260 | 0.14 | 8.2 | acrylate | 62.5 |
| *INO* | Intrinsically photosensitive | 6.7 | 1366 | 0.24 | 4.3 | acrylate | 62.5 |
| *FiberCore* | SM1500 (4.2/125) | 4.2 | 1450 | 0.29 | 3.8 | acrylate | 62.5 |
| *Nufern* | UHNA3 | 3.3 | 900 | 0.35 | 2.0 | acrylate | 62.5 |
| *Spectran* | Photosensitive Fiber Prototype | 3.7 | na | 0.30 | na | acrylate | 62.5 |
| *FiberLogix* | High NA fiber | 4.3 | 1400 | 0.28 | 3.8 | polyimide | 10 |
| *OFS* | Clearlite Poly 1310 21 | 5.8 | 1290 | 0.21 | 4.7 | polyimide | 15 |

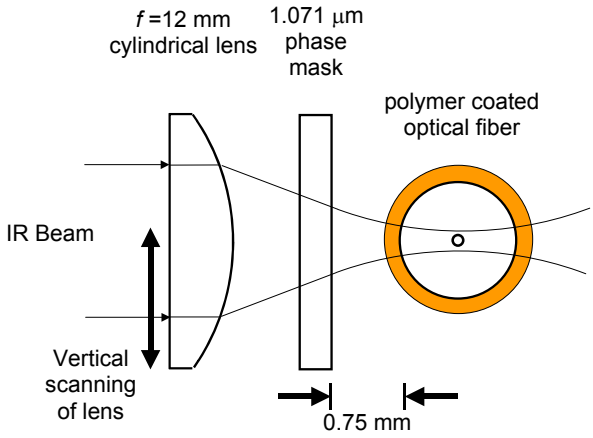


Fig. 1 Schematic representation of lens-fiber-phase mask geometry for FBG fabrication in standard optical fibers.

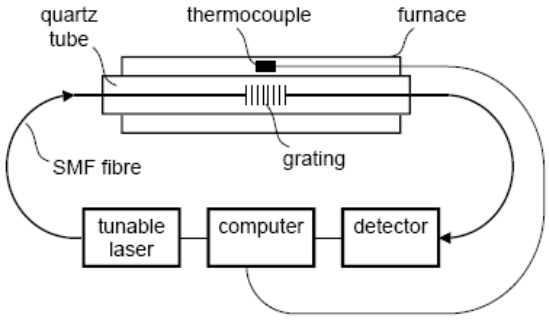


Fig. 2 High temperature long term stability measurement set-up for FBGs written in single mode fiber

The FBGs were made in both pristine fibers and those loaded with high-pressure hydrogen gas at 23 °C and 2400 psi for 240 hours. Exposures were made using 125 fs autocorrelated pulses of 800 nm IR radiation from a Ti:sapphire amplifier at a repetition rate of 100 Hz. A cylindrical lens with a focal length $f$ = 12 mm was used to focus the 6.4 mm diameter IR beam through the phase mask and coating into the fiber core. Assuming Gaussian beam optics, the focal spot and the Rayleigh range in the absence of the fiber are approximately 2 and 4 mm, respectively. The fibers were positioned ~ 750 μm behind the 1.07 μm pitched phase mask, resulting in the formation of a two-beam interference pattern at the fiber core [14]. For a uniform core exposure, the focused beam was continually scanned perpendicular to the fiber's axis in a direction parallel to the phase mask grooves ± 10 μm about the fiber core every 20 seconds. A schematic of the exposure set up is shown in Fig. 1. With this focusing geometry, pulse energies greater than 440 μJ resulted in damage to the acrylate polymer coating. When using the same exposure conditions on polyimide coated fiber, lower pulse energies up to 180 μJ could be used before damage to the coating was visible. The intensities used here are consistent with formation of type I-IR gratings in hydrogen loaded *SMF-28* fiber [15, 16]. Transmission spectra were obtained during the exposure using an $Er^{+}$ fiber white light source and an optical spectrum analyser.

In order to understand their absorptive properties, low signal absorption scans of typical acrylate and polyimide coatings were performed using a *Cary 3*UV-Visible spectrophotometer. *Desolite 950-200* optical fiber recoating acrylate from *DSM Desotech Inc.,* was used to prepare 7 μm thick films by sandwiching the acrylate between two silica windows and then UV curing for 1 minute. Freestanding films of the polyimide coatings used by the fiber manufacturers were unavailable. Instead, *Kapton 30H* polyimide films from *Dupont* with 7.5 μm thickness were measured.

Long-term stability tests were performed in a Lindberg tube furnace equipped with an internal quartz tube of 2.54 cm diameter centered within the furnace tube shown schematically in Fig. 2. Gratings were loosely placed in the inner tube so that no external stresses were applied to the grating. The temperature in close proximity to the grating was monitored using a thermocouple probe with automated data logging, in addition to the thermocouple built into the furnace's feedback and control circuit. The experiments were performed in ambient air and the heating rate was limited to 10 °C $min^{-1}$. A swept tunable laser system was used to measure the grating spectral responses. During the experiments, the grating spectra and furnace temperature were measured and recorded every 5 minutes. A swept tuneable laser system was used to continually measure the grating spectral responses.

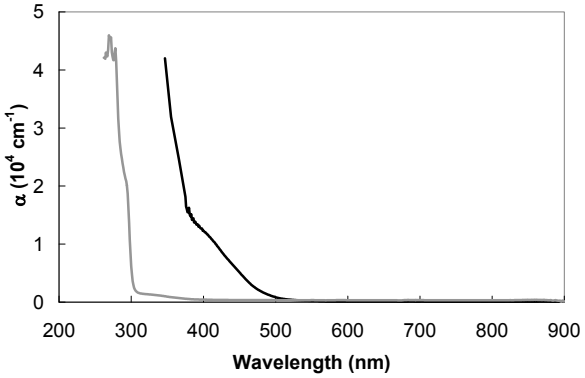


Fig. 3 Measurement of the absorption coefficient a of a 7.5 μm thick film of the polyimide *Kapton 30H* (black trace) and a 7 μm thick film of DeSolite 950-200 acrylate film (grey) as measured with a UV-visible spectophotometer. No transmitted signal was observed through the film below 375 nm and 260 nm for the polyimide and acrylate films respectively.

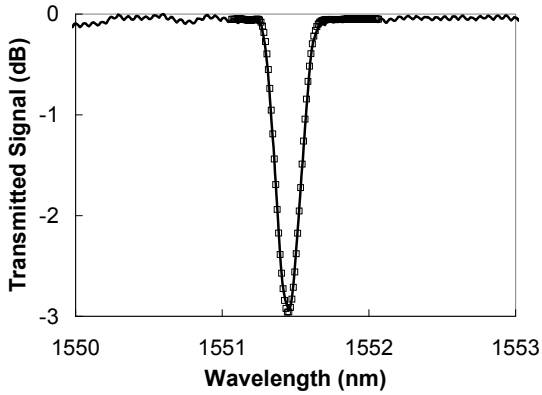


Fig. 4 Transmission spectrum of an FBG written through the jacket of SMF-28 fibre with 800 nm, 125 fs, 250 μJ pulses, focused with a *f*=19 mm cylindrical lens and a 1.071 μm pitched phase mask. Overlaid modelled spectrum shown with open squares.

## 3. RESULTS AND DISCUSSION

### 3.1 UV, IR absorption studies of Acrylate and Polyimide

Figure 3 presents the absorption coefficient α versus wavelength of the 7μm thick *DeSolite* 950-200 acrylate film and the 7.5 μm thick *Kapton 30H* polyimide film. The thickness of the polyimide films deposited on the optical fibers is typically twice that of the Kapton film measured here. The signal transmission below 500 nm was significantly attenuated with no transmission detectable by the spectrophotometer below 375 nm. For the acrylate film, high transmission is observed above 300 nm, but no detectable transmission using the spectrophotometer is observed below 260 nm. Polyimide is well known to have an extremely large α or alternatively an extremely thin 1/e absorption depth at wavelengths used for UV grating inscription. For polyimide, $\alpha = 2.6 \times 10^5$ cm$^{-1}$ at 248 nm [17] while the a of acrylate resins used for fiber coatings are an order of magnitude lower equaling $2.5 \times 10^4$ cm$^{-1}$ at the same wavelength [18]. For *SMF-28* fiber, the α of the acrylate coating at 248 nm was shown to be $4.6 \times 10^4$ cm$^{-1}$ [19]. The acrylate coatings have an approximately 5 to 10 times lower absorbance in the UV than the same thickness of polyimide at these wavelengths. The absorption spectra presented in Fig.3 are consistent with these values. It is not obvious that established techniques for inscription of gratings through an acrylate jacket would still be successful with a polyimide coating. From Fig. 3 it is seen that polyimide is transparent to low signal IR radiation, however the absorption bands in the polymer that are accessed by UV photon energies can also be accessed through multiphoton absorption of higher intensity infrared pulses.

### 3.2 Through the coating FBG inscription in standard telecom fiber

Bragg gratings were first written in acrylate coated SMF-28 fibers that were hydrogen loaded. The transmission spectrum of a grating written in hydrogen loaded SMF-28 with pulse energies of 250 μJ is presented in Fig. 4. The total exposure time for the grating inscription was ~ 5 minutes, after which no further grating growth was observed. For SMF-28 fiber, the Type I-IR induced index change has been shown to be a 5-photon process [16]. Using the Rouard method [20], the transmission spectrum of the grating was modelled assuming a Gaussian index profile 6.4 mm in length and a 5-photon process. The modelled response is shown as the dotted line in Fig. 4. From the model, the maximum index modulation corresponding to the experimental data is $\Delta n = 2.2 \times 10^{-4}$.

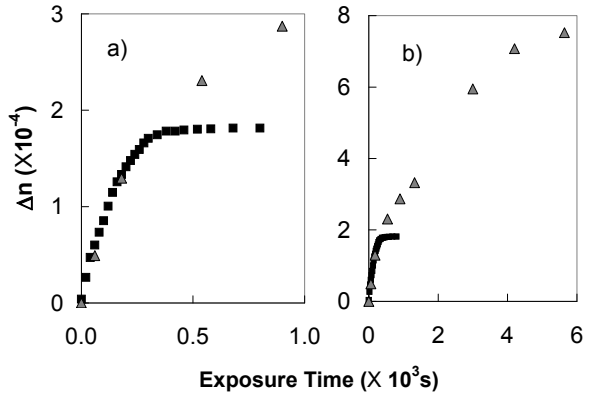


Fig. 5 a) Increase in Δn as a function of exposure time for gratings written through the acrylate coating of $H_2$ –loaded *SMF-28* fiber with 250 μJ pulses and a *f*=19 mm cylindrical lens (black squares) and with the coating removed (gray triangles); b) Long term continued grating growth on stripped SMF-28 fiber.

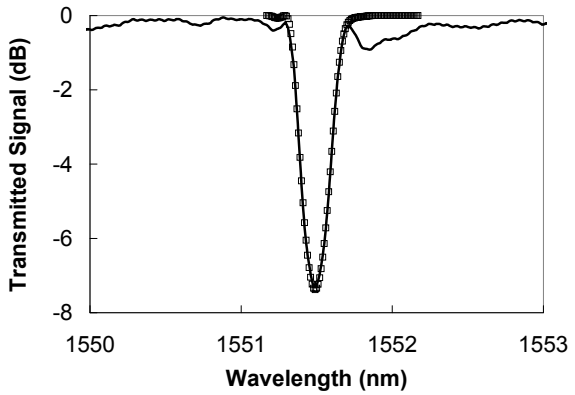


Fig. 6 Transmission spectrum of an FBG written through the jacket of SMF-28 fiber with 800 nm, 125 fs, 400 μJ pulses, focused with a *f*=12 mm cylindrical lens and a 1.071 μm pitched phase mask. Overlaid modelled spectrum shown with open squares.

Under identical exposure conditions (100 Hz, 20 s cycle of ± 10 μm beam sweep) and pulse energies of 220 μJ, grating growth as a function of time was compared for gratings written through the jacket and with the jacket chemically removed. In Fig. 5 a), significant growth is initially observed for the grating written through the jacket however after ~ 5 minutes exposure, no further change in Δn is observed. In the case of the stripped fiber, grating growth does not stop but continues even after exposure to the laser for 90 minutes (see Fig. 5 b). Observation of the exposed region of the polymer jacket under an optical microscope revealed some damage to the jacket at the fiber cladding-jacket interface, but no damage to the jacket surface. Several femtosecond IR laser-based ablation studies of polymeric materials have shown that the threshold for induced index change and ablation of the polymer decrease with the number of incident pulses [21, 22]. It is likely then that the first several hundred pulses are inducing 'incubation sites' in the acrylate polymer coating that eventually reduces the transmission of the IR radiation through the jacket thus limiting the Δn growth.

Using the 12 mm focal length lens, a stronger grating could be written before incubation sites in the jacket attenuated the incident beam. The transmission and modelled spectra are shown in Fig. 6. Compared to the modelled spectrum, the Δn achieved with this tighter focusing geometry was $3.5 \times 10^{-4}$.

To study the reliability of these gratings, 5 devices were made using the same recipe as for the grating shown in Fig. 4 (*f* = 19 mm). Using an optical fiber pull tester (Vytran PTR-100), the breakage strength was compared with pristine SMF-28. For the 5 devices, the breakage strength was 4.5 ± 0.5 GPa (690 ± 80 kPSI) as compared with 5.3 ± 0.3 GPa (770 ± 40 kPSI) for the pristine fiber. The high Δn grating shown in Fig. 6 (f = 12 mm) was also pull tested and had a slightly lower breakage strength of 4.1 GPa. Compared with the reliability of femtosecond gratings written through the jacket by the point-by-point technique [9], a 2 to 3-fold increase in pull test strength is realized which is approaching that of the pristine fiber. As the induced index change of the gratings presented here is not the result of a plasma formation and micro-void generation, as in [13], but is more likely a result of defect formation and compaction, the grating reliability is not compromised by embrittlement due to the formation of micro-cracks and micro-voids.

### 3.3 Bragg Gratings in Hydrogenated acrylate coated high NA Fibers

Exposure pulse energies up to 440 μJ could be used resulting in sufficient intensities in the fiber core for FBG formation. Higher pulse energies directly damaged the coating causing a reduction in transmission of the writing beam through the fiber before significant grating growth was achieved.

Exposure through the coating of $H_2$-loaded *SM1500* and *INO* fibers at 440 μJ/pulse resulted in rapid initial Δ*n* growth followed by a saturation in the Δ*n* (inset Fig. 7). The Δ*n* values were determined from the FBG spectra using commercial

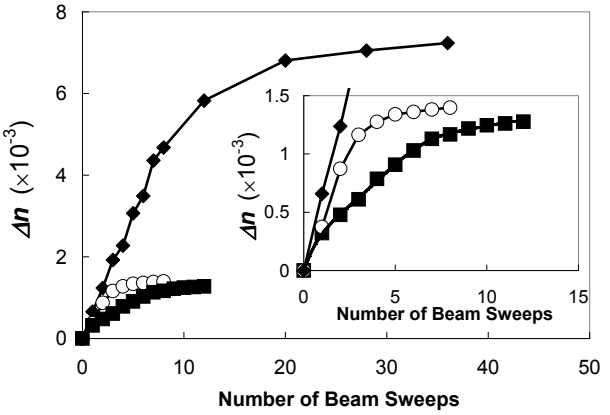


Fig. 7. Grating growth of $H_2$-loaded SM1500 (white circles) and INO fiber (black squares) while being exposed to fs IR radiation through the acrylate coating, and grating growth for $H_2$-loaded SM1500 without the polymer coating (black diamonds). Short-term growth is displayed in the inset plot.

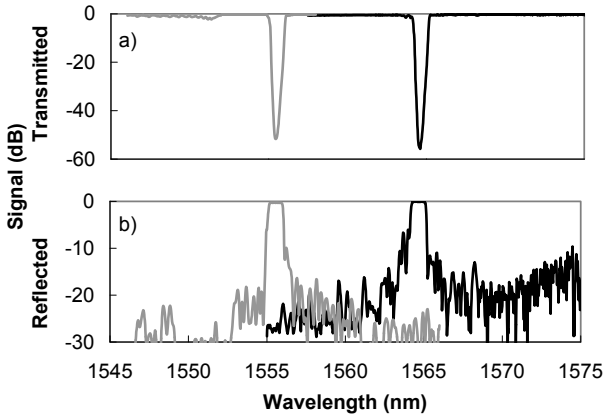


Fig. 8. a) Transmission and b) reflection spectra of saturated gratings written through the jacket of H2-loaded SM1500 fiber (black) and INO fiber (gray).

software and assuming a uniform FBG with a 6.4 mm long Gaussian apodization profile and a sinusoidal variation of the $\Delta n$. The $\Delta n$ growth of the two fibers is different, with the growth of the *INO* fiber reaching the saturation level at twice the accumulated exposure as compared to the *SM1500* fiber. Saturated $\Delta n$ levels of the *SM1500* and *INO* fiber were 1.4 $\times$ $10^{-3}$ and 1.3 $\times$ $10^{-3}$ respectively. Although the Ge concentration is significantly larger in the *SM1500* fiber, the difference in the saturated $\Delta n$ levels of the two fibers is relatively small. The saturated $\Delta n$ level of the *INO* fiber is ~ 85% of that of the *SM1500* fiber.

Compared to the Bragg resonance ($\lambda_B$) of FBGs made in *SMF-28* with the same phase mask ($\lambda_B$ = 1549.8 nm), the $\lambda_B$ values for the *SM1500* and *INO* fibers were shifted to longer wavelengths by ~15 nm and ~5 nm, respectively. The red shifts in $\lambda_B$ result from the high Ge content in the fiber cores. Using the Bragg relation for FBGs ($\lambda_B = 2n_{eff}\Lambda$, where $\Lambda$ is the FBG pitch), the $n_{eff}$ for the *SM1500* and *INO* fibers were 1.46 and 1.453, respectively, corresponding to an increment of 1% and 0.4% of the respective $n_{eff}$'s when compared to the *SMF-28*. This increase is likely proportional to the variations in the Ge concentration of the two fibers cores as compared to *SMF-28* if the core geometry differences are ignored.

Spectra of saturated gratings written through the coatings of *SM1500* and the *INO* fibers are shown in Fig. 8a and b, respectively. The grating spectra are of reasonable quality although the reflection noise floor level is higher when compared to FBGs written without the coating under the same exposure conditions and to the same $\Delta n$. The increased noise floor level may result from a non-uniform IR transparency of the acrylate coating along the beam exposure length.

From Fig. 7, the grating growth is much higher when identical exposure conditions are applied but with the *SM1500* fiber coating removed. The saturated $\Delta n$ level is almost five times larger than when the coating is present. To achieve the same coated-fiber saturated $\Delta n$ value of 1.4 $\times$ $10^{-3}$, but with the fiber coating removed, the laser pulse energy was reduced from 440 μJ to ~200 μJ. This reduction can be taken as a measure of the acrylate coating attenuation combined with the beam distortion through the coating as a result of the coating non-uniformity. In fs IR laser ablation studies of polymers, the damage threshold decreases with the number of incident pulses [22] The first several hundred pulses are likely inducing 'incubation sites' in the polymer coating that eventually reduces the transmission of the IR radiation through the jacket thus limiting the $\Delta$n growth.

The same coating attenuation was seen in grating formation threshold measurements made in the *SM1500* fiber. Whereas a very small reflectivity grating was written with an energy level of 140 μJ/pulse through the coating, grating formation was observed at ~ 90 μJ/pulse when the coating was removed.

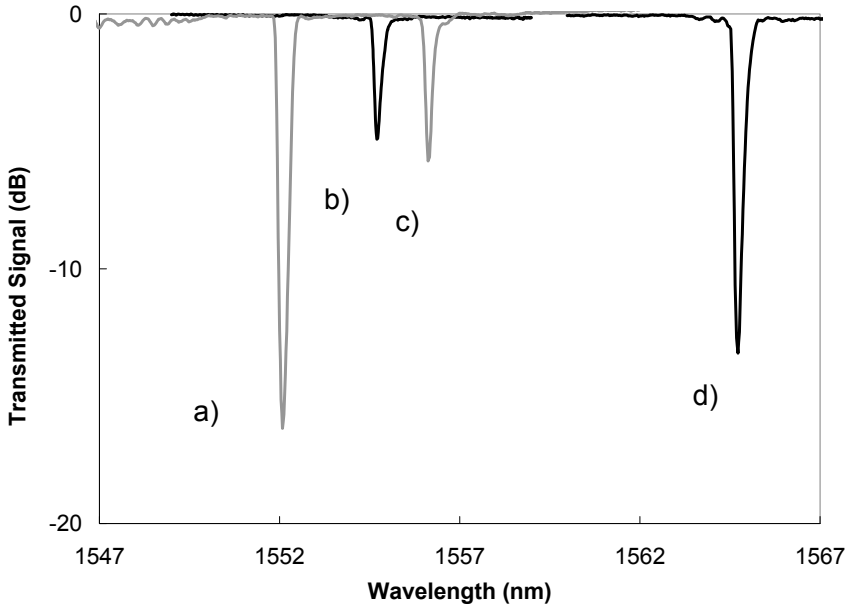


Fig. 9. Transmission spectra of saturated gratings written through the jacket of unloaded a) boron-codoped high-NA *Spectran* fiber, b) *INO* fiber, c) *UHNA3* fiber, and d) *SM1500* fiber.

### 3.4 FBGs Written Through Acrylate Coating in Unloaded High NA Fibers

Under the same exposure conditions, 440 μJ/pulse at 200 Hz, FBGs were written through the coatings of the *SM1500*, *INO, UHNA3*, and the *Spectran* prototype fibers without $H_2$-loading. The *SM1500* fiber was exposed for 5 minutes and resulted in a saturation $\Delta n$ level of $7 \times 10^{-4}$ corresponding to a 14 dB strong grating (Fig. 9d). FBGs written in the *INO* and *UHNA3* fibers produced lower levels of saturated index change, namely $3 \times 10^{-4}$ and $4 \times 10^{-4}$, respectively, with transmission losses of –4.9 and –5.8 dB, respectively (Fig 9b and 9c). The *Spectran* prototype fiber showed the highest saturated $\Delta n$ level of $8 \times 10^{-4}$ corresponding to a 16 dB strong grating (Fig. 9a).

For unloaded fiber, the difference in fiber photosensitivities and saturated $\Delta n$ is dependent upon the germanium concentration in the fiber core. For $H_2$-loaded fibers, much higher photosensitivity is seen; however, the disparity in saturated $\Delta n$ with Ge core concentration is reduced. To increase the $\Delta n$ induced in unloaded fibers, a tighter focusing arrangement of the laser beam is required. The results presented here refer to optical fibers with high NA. If for some applications the value of the splicing loss between these fibers and *SMF-28* is too large, then boron-codoped fibers similar to the *Spectran* prototype fiber, are commercially available.

To study the reliability of the gratings, six devices were inscribed through the jacket using the *SM1500* fiber. Using an optical fiber pull tester (Vytran PTR-100), we compared the breakage strength with pristine *SM1500* and *SMF-28* fiber. As a result of fiber availability, only a limited number of pull tests could be performed. For the devices tested, the breakage strength was 4.2 ± 0.5 GPa ($610 \pm 80 \times 10^3$ psi) as compared with 5.5 ± 0.3 GPa ($790 \pm 40 \times 10^3$ psi) for the pristine fiber. Little degradation in the fiber physical strength as a result of the Bragg gratings inscription is shown. Reduction in breakage strength is similar to that for gratings written through the jacket in *SMF-28* fiber.

### 3.5 FBGs written through the jackets of Polyimide coated fibers

Exposure pulse energies up to 180 μJ could be used before the deterioration of the polyimide fiber coating was observed. In the absence of $H_2$-loading, the maximum FBG reflectivity that was achievable before coating damage was ~ 1%. A reflection spectrum of a device made in the *OFS* fiber is shown in Fig. 10. In the case of the acrylate-coated fiber, pulse

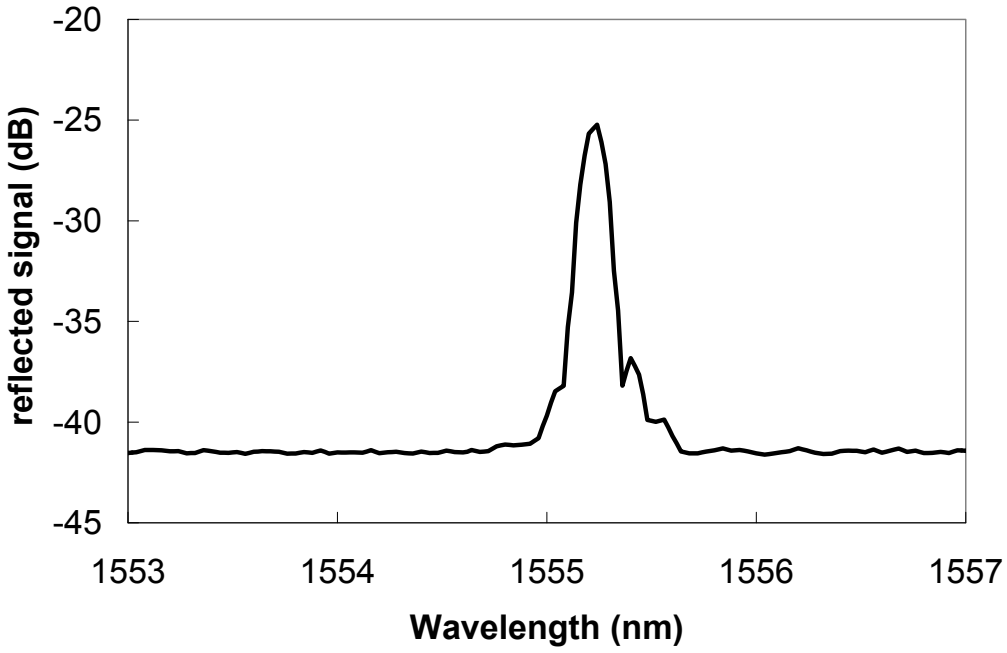


Fig. 10. Reflection spectrum of an FBG written through the polyimide jacket of the *OFS* fiber without $H_2$-loading

energies a factor of two higher (up to 440μJ with the same focusing geometry) could be employed to inscribe the grating before coating damage was observed. The lower absorption of the acrylate coating to fs-IR radiation, compared to that of the polyimide coatings, facilitated the inscription of a stronger Bragg grating. The transmission spectrum of the grating written in the unloaded *Fibercore* fiber is presented in Fig 9d). The observed transmission loss of the device at the Bragg resonance was –13 dB, which represented a 95% reflectivity.

When hydrogen loaded, much higher reflectivity gratings could be written through the polyimide-based jackets of both the *OFS* and *Fiberlogix* fibers. The total exposure time for the grating inscription in each fiber was ~ 5 minutes, after which no further grating growth was observed. From the transmission spectra shown in Fig. 11a) and b), the reflectivities and Bragg resonances, $\lambda_B$, of the 6.4 mm long *OFS* and *Fiberlogix* fiber gratings were –3.5 dB (55%), –1.8 dB (34%) respectively and $\lambda_B$ = 1555.8 and 1559.7 nm respectively. According to the Bragg relation for FBGs, $\lambda_B = 2n_{eff}\Lambda$, where $\Lambda$ is the FBG pitch and $n_{eff}$ is effective core mode index. The post exposure $n_{eff}$ for the *OFS* and *Fiberlogix* fibers were then 1.453 and 1.456, respectively. Similar FBGs written in *Corning SMF-28* fiber result in an $n_{eff}$ = 1.447. The red shift in the $\lambda_B$ of the *Fiberlogix* FBG when compared to that of the *OFS* and *SMF-28* FBGs is likely a result of higher Ge content in the high NA fiber cores compared to the SMF-28 fiber core if the core geometry differences are ignored.

For both the loaded and unloaded grating inscriptions, the induced index change occurred in the low intensity regime (type I-IR), which has been associated with defect formation/material compaction. To model the grating response, a commercial software package employing coupled mode theory from *Apollo Photonics* was used, taking into account the $n_{eff}$ of the fiber as well as the overlap between the mode field diameter and the core diameter. When not given, the core diameter $d$ was estimated using the expression:

$$d = \frac{V_c \lambda_c}{\pi NA} \tag{1}$$

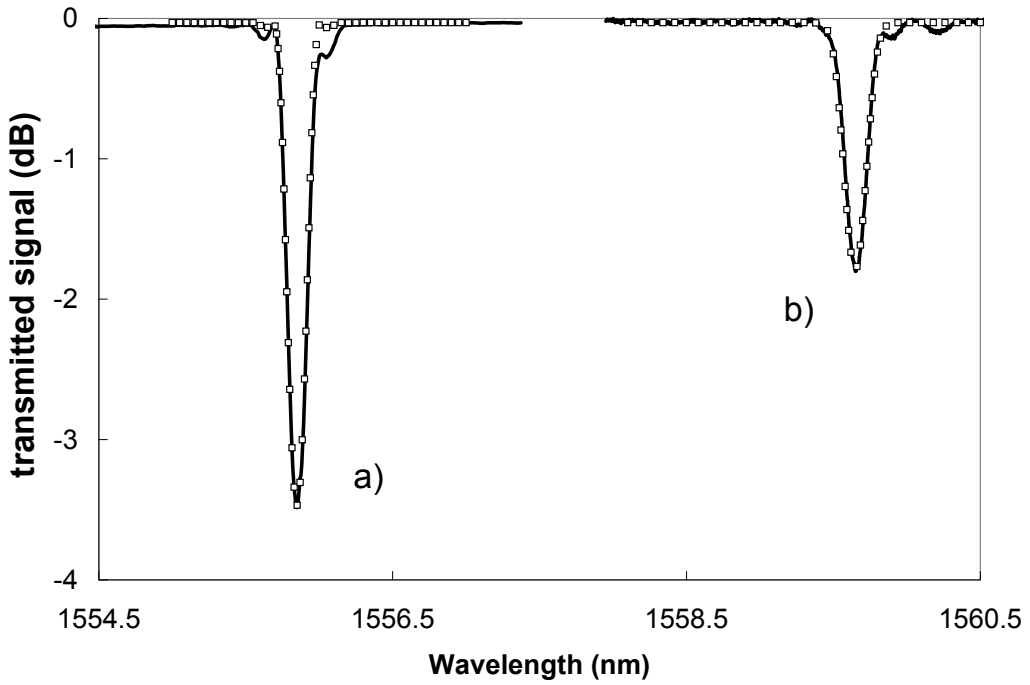


Fig. 11. Transmission spectra of FBGs written through the polyimide jacket of $H_2$-loaded a) *OFS* and b) *Fiberlogix* fibers. Overlaid modeled spectra shown with white dots.

where $V_c = 2.4$ is the normalized cut off frequency of the $LP_{11}$ mode, and $\lambda_c$ is the cut off wavelength. In the commercial package, the $\Delta n$ is assumed to be sinusoidal however for *SMF-28* fiber, the Type I-IR induced index change has been shown to be a 5-photon process [16]. For a given reflectivity, the value of the $\Delta n$ generated by the software package assuming a sinusoidal profile rather than a profile that varies with the fifth power of the intensity, tends to be modestly underestimated [20]. The modelled grating responses are denoted by white squares in Fig. 2b) and 3. From the model, the $\Delta n$ values for gratings written in the *Fibercore, OFS* and *Fiberlogix* fibers were 7, 1.6 and $1.4 \times 10^{-4}$ respectively. For the case of the unloaded *OFS* fiber, the 1 % reflectivity corresponds to an $\Delta n = 3 \times 10^{-5}$.

Observation of the exposed region of the polyimide polymer jacket under an optical microscope revealed some damage to the jacket surface after the 5-minute exposure. Femtosecond-IR laser machining studies of polyimide have shown that the ablation threshold for polyimide decreases with the number of incident laser pulses [21]. As with the acrylate coating, it is likely that prolonged exposure of the polyimide jacket to the incident fs-IR pulsed radiation induces 'incubation sites' in the polymer that results in increased absorption that eventually reduces the transmission of the IR radiation through the jacket thus limiting the $\Delta n$ growth.

Interestingly, the apodisation profiles of the modelled data that best fit the experimental transmission spectra were different for each of the fiber coatings. The apodisation function is given by [23]:

$$\Delta n(z) = n_{\max} \exp\left[ - A \left( \frac{|z - z_0|}{L} \right)^B \right] \tag{2}$$

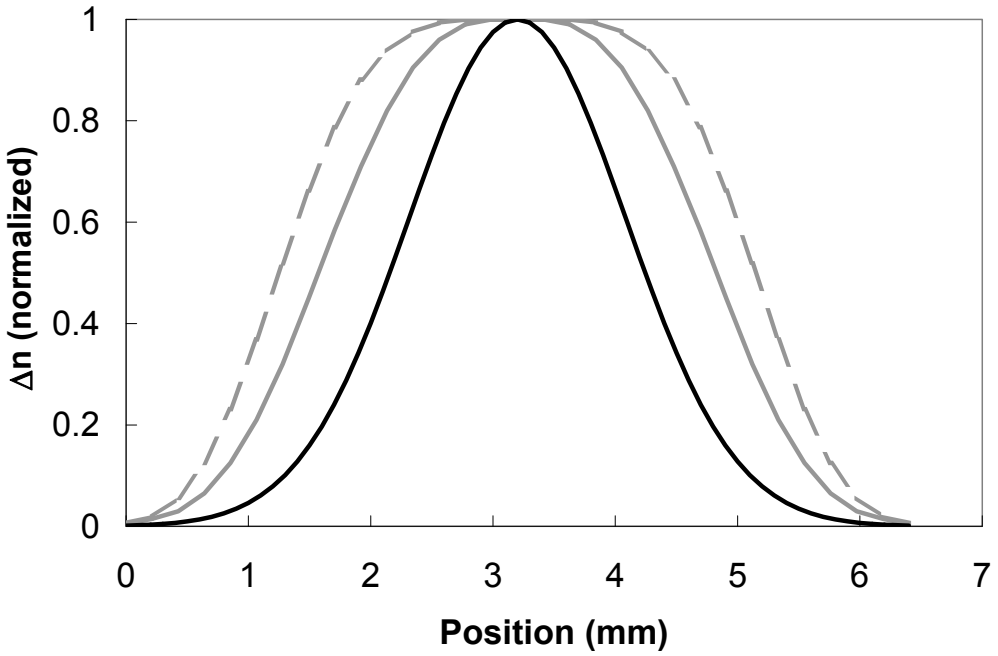


Fig. 12. Apodisation profiles used to model the spectral data. The black, grey and grey dotted traces are the profiles used for the *Fibercore, Fiberlogix* and *OFS* fibre grating spectra respectively..

where $\Delta n(z)$ is the index modulation along the grating length $L$, $n_{max}$ is the maximum $\Delta n$ and $z_0$ is the position of the maximum index change. $A$ is the Gaussian window parameter which is equal to 5, while $B$ is a positive parameter. For a simple Gaussian apodisation, $B = 2$. For the acrylate-coated fiber, the apodisation profile fit a simple Gaussian apodisation, similar to that of the incident beam. For the polyimide-coated fibers, the more intense portions of the incident beam were attenuated resulting in super-Gaussian type grating apodisation profiles. The modelled grating apodisation profiles, which resulted in the best fit to the spectral responses for each of the fibers, are shown in Fig. 12.

To study the FBG temperature stability, isochronal/isothermal annealing studies were performed on the polyimide-coated gratings at elevated temperatures. In Fig. 13, the reduction of $\Delta n$ at various elevated temperatures is shown for a grating made through the jacket of the *OFS* fiber with an initial $\Delta n$ of $1.2 \times 10^{-4}$. A portion of the $\Delta n$ is rapidly annealed out at 200 °C but the remaining $\Delta n$ is relatively stable with increasing temperature up to 400 °C. After 16 hours at 400 °C, the grating $\Delta n$ stabilized at a value of $6.5 \times 10^{-5}$. When the fiber temperature was further increased in 100 °C increments from 400 °C and annealed for 1 hour at each temperature, grating erasure was observed with complete grating erasure occurring at 800 °C. In a separate experiment, another device was annealed at 360 °C for 140 hours after being pre-annealed at 75 °C for 36 hours in order to out-gas any remaining hydrogen (inset Fig. 13). After 140 hours, a $\Delta n \approx 7.3 \times 10^{-5}$ remained.

Isochronal/isothermal curves for a device made in the *Fiberlogix* fiber are shown in Fig 14. The device was left at room temperature for 1 month in order to outgas all of the hydrogen after the grating inscription. In Fig. 14a) the isochronal annealing curve is shown where the device is annealed for one hour at 250, 300, 400 and 500 °C and then is allowed to remain at 500 °C for a further 115 hours (Fig 14 b). The grating reflectivity after the 115 hours was –0.38 dB (8%), which corresponds to an $\Delta n \approx 6 \times 10^{-5}$ that is ~ 60% of the initial $\Delta n$ value. Increasing the temperature to 600 °C resulted in steady and complete erasure of the device after a further 65 hours of annealing. Comparing the annealing characteristics of the *OFS* and *Fiberlogix* FBGs, a more thermally stable $\Delta n$ could be induced through the coating of the *Fiberlogix* fiber. With its higher Ge-dopant core concentration, the *Fiberlogix* FBG was stable up to 500 °C as opposed to 400 °C for the *OFS* FBG. As the rated operating temperature of both the *OFS* fiber *Pyrocoat* jacket and the

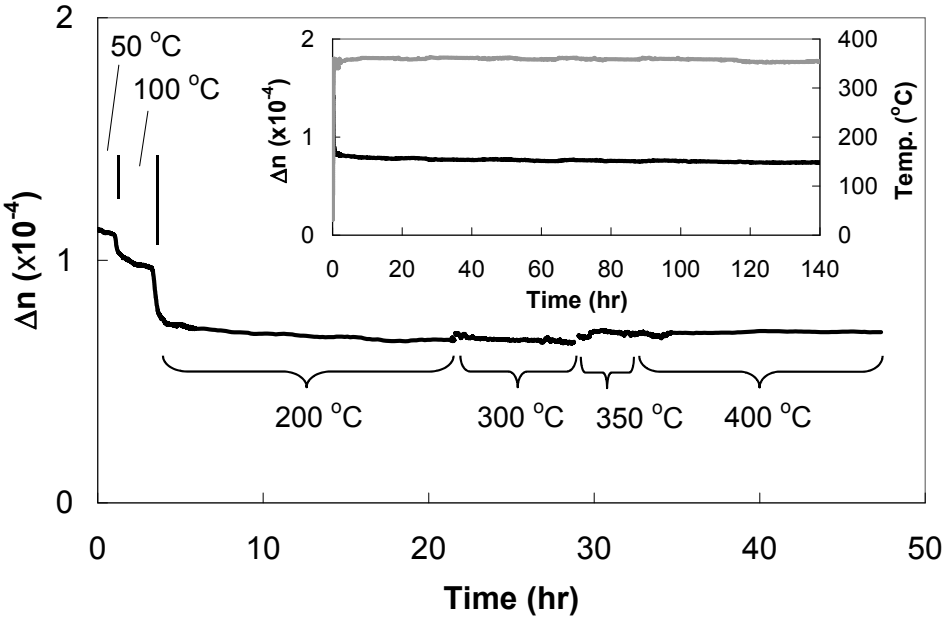


Fig. 13. Isochronal annealing study of a FBG in the polyimide coated OFS fibre. Inset figure is the long-term isothermal annealing study at 360 °C of a FBG in OFS fibre with Δn and temperature denoted by black and gray traces respectively.

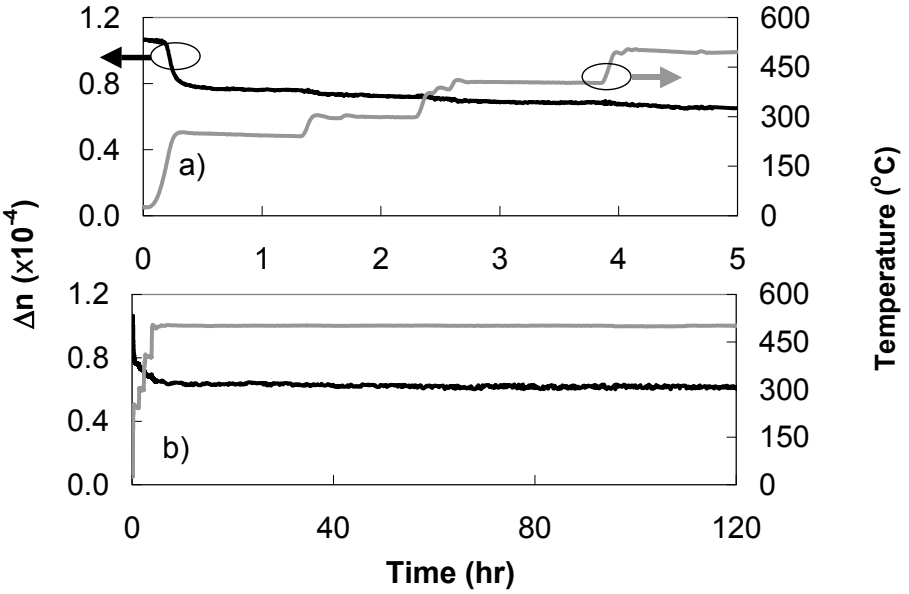


Fig. 14. a) Isochronal and b) isothermal annealing study of a FBG written through the polyimide coating of the *Fiberlogix* fibre. Index modulation and temperature denoted by black and gray traces respectively.

*Fiberlogix* polyimide jacket are 300 °C, significant grating index modulations could be induced through the jacket of either fiber that would remain stable within the operating temperature of the coating.

To study the reliability of the gratings, 12 devices were inscribed through the polyimide jacket of the *Fiberlogix* fiber. Using the Vytran optical fiber pull tester, we compared the breakage strength with pristine *Fiberlogix* fiber. As a result

of fiber availability, only a limited number of pull tests could be performed. For the devices tested, the breakage strength was 2.8 ± 0.3 GPa (399 ± 49 × $10^3$ psi) as compared with 5.8 ± 0.3 GPa (835 ± 40 × $10^3$ psi) for the pristine fiber.

An important application for the polyimide coated FBG devices presented here would be for the oil and gas industry as fiber optic sensors to monitor the downhole environment. As such, the sensors would be exposed to hydrogen partial pressures greater than 1 atmosphere at temperatures above 100 °C. Operation in such an environment has been shown to result in $H_2$-induced absorptive losses in the optical fiber, both due to the presence of $H_2$ and because of the reaction of hydrogen with defects in the fibers [24]. The use of hydrogen loading to increase fiber photosensitivity for grating inscription does not contribute to these high temperature induced losses when deuterium is replaced by hydrogen in order to increase the fiber photosensitivity. Laser induced losses near the telecom window at 1.38 μm due to the formation of OH are shifted to longer wavelengths outside the window when deuterium is used. As devices are typically manufactured at room temperature, unreacted gas diffuses out of the fiber.

## 4. CONCLUSIONS

The technique of through-the-jacket inscription of fiber Bragg gratings using femtosecond infrared laser radiation and a phase mask has been presented. Bragg gratings have been inscribed directly through both acrylate and polyimide polymer coatings of standard commercially available optical fibers that in some instances had their photosensitivity to ultrafast IR radiation enhanced through the process of hydrogen-loading. Fiber pull tests of written gratings in acrylate coated fibers resulted in fiber strengths close to that of the pristine fiber while devices fabricated in polyimide coated fiber maintained ~50% of the pristine fiber pull test strength.

Depending on the levels of Ge-doping in the fibers and whether or not the fibers were hydrogen loaded, grating inscription in the fiber core resulted in large refractive index modulations. For fibers with the highest germanium content, hydrogen-loaded and unloaded index modulations of ~ $1.4 \times 10^{-3}$ and $7 \times 10^{-4}$ were obtained respectively.

Fiber Bragg gratings that are inscribed directly through the polyimide polymer coating of commercially available optical fibers are also reported. Gratings made in hydrogen loaded high NA fiber have index modulations of greater than $1 \times 10^{-4}$ that maintain ~60 % of their initial strength after annealing for 120 hours at 500 °C. Gratings with better thermal stability were induced in fibers possessing higher Germanium doping levels.

Although presently more of a research tool than an industrial laser, the high-powered femtosecond infrared laser is proving itself to be a versatile instrument for grating inscription in various waveguides and materials. Structures can be successfully inscribed in or through any material that is transparent to low signal 800 nm infrared radiation. For this reason femtosecond IR radiation is ideal for through-the-jacket inscription of gratings, especially for jacket materials that are highly absorbing in the UV such as polyimide. Near UV pulsed sources such XeCl (308 nm) or XeF (351 nm) excimer laser systems, or frequency tripled Nd:YAG systems (355 nm) are used extensively for laser machining of polyimide in the microelectronics industry due to the high absorption of polyimide at these wavelengths [25]. It is therefore unlikely that such systems could inscribe a grating through the polyimide coating of an optical fiber.

The presented method is a very straightforward solution for applications requiring Bragg grating inscription in the core of optical fibers without the need of fiber coating removal. The method does not require special coatings nor custom fiber designs but allows for the inscription of very low- to very high-reflectivity Bragg gratings after a few seconds exposure with simple alignment similar to standard UV laser Bragg grating inscription techniques. Such gratings when inscribed through high temperature stable polymer coatings are suitable for high temperature sensors used for downhole monitoring in the oil and gas industry.

## 5. ACKNOWLEDGEMENTS

We would like to thank Tom Graver of Micron Optics, Alexis Mendez of MCH Engineering and Rogerio Ramos of Insensys Oil and Gas for their valuable discussions and contributions.

## REFERENCES


[1] Kersey, A. D., Davis, M. A., Patrick, H. J., LeBlanc, M., Koo, K. P., Askins, C. G., Putnam, M. A., and Friebele, E. J., "Fiber grating sensors," J. Lightwave Tech. **15** (8), 1442-1463 (1997).

[2] Hill, K. O. and Meltz, G., "Fiber Bragg grating technology fundamentals and overview," J. Lightwave Tech. **15** (8), 1263-1276, 1997.

[3] Friebele, E. J., Putnam, M. A., Askins, C. G., Jomrighaus, Z. J., Mack, W. D., and Smith, G. A., "Method for recoating optical fibers with polyimide," Electron. Lett. **34** (12), 1249-50, 1998.

[4] Starodubov, D. S., Grubsky, V., and Feinberg, J., "Efficient Bragg grating fabrication in a fiber through its polymer jacket using near-UV light," Electron. Lett. **33** (15), 1331-3, 1997.

[5] Imamura, K., Nakai, T., Moriura, K., Sudo, Y., and Imada, Y. "Mechanical strength characteristics of tin-codoped germanosilicate fiber Bragg grating by writing through UV-transparent coating," Electron. Lett. **34** (10), 1016-1017, 1998.

[6] Espindola, R. P., Atkins, R. M., Simoff, D. A., Nelson, K. T., and Paczkowski, M. A. "Fiber Bragg gratings written through a fiber coating," in Optical Fiber Communications Conference. Dallas, 1997, pp. PD-4.

[7] Gu, X., Guan, L., He, Y., Zhang, H. B., and Herman, P. R. "High-Strength Fiber Bragg Gratings for a Temperature-Sensing Array," IEEE Sens. J. **6** (3), 668-671, 2006.

[8] Chao, L., Reekie, L., and Ibsen, M. "Grating writing through fiber coating at 244 and 248 nm," Electron. Lett. **35** (11), 924-926, 1999.

[9] Martinez, A., Khrushchev, I. Y., and Bennion, I., "Direct inscription of Bragg gratings in coated fibers by an infrared femtosecond laser," Opt. Lett. **31** (11), 1603-1605, 2006.

[10] Mihailov, S. J., Grobnic, D., and Smelser, C. W., "Efficient grating writing through fiber coating with femtosecond IR radiation and phase mask," Electron. Lett. **43** (8), 442-443, 2007.

[11] Grobnic, D., Mihailov, S.J., Smelser, C. W., and Ramos, R. T., "Ultrafast IR Laser Writing of Strong Bragg Gratings Through the Coating of High Ge-Doped Optical Fibers," IEEE Photon. Technol. Lett. **20** (12), 973-975, 2008.

[12] Mihailov, S. J., Grobnic, D., Walker, R. B., Smelser, C. W., Cuglietta, G., Graver, T. and Mendez, A., "Bragg grating writing through the polyimide coating of high NA optical fibers with femtosecond IR radiation," Opt. Comm. **281** (21), 5344-5348, 2008.

[13] Martinez, A., Dubov, M., Khrushchev, I., and Bennion, I., "Photoinduced Modifications in Fiber Gratings Inscribed Directly by Infrared Femtosecond Irradiation," IEEE Photon. Technol. Lett. **18** (21), 2266-2268, 2006.

[14] Smelser, C. W., Grobnic, D., and Mihailov, S. J., "Generation of pure two-beam interference grating structures in an optical fiber with a femtosecond infrared source and a phase mask," Opt. Lett. **29** (15), 1730-1732, 2004.

[15] Smelser, C. W., Mihailov, S. J., and Grobnic, D., "Hydrogen loading for fiber grating writing with a femtosecond laser and a phase mask," Opt. Lett. **29** (18), 2127-2129, 2004.

[16] Smelser, C. W., Mihailov, S. J., and Grobnic, D., "Formation of Type I-IR and Type II-IR gratings with an ultrafast IR laser and a phase mask," Opt. Exp. **13** (14), 5377-5386, 2005.

[17] Koren G., and Yeh, J. T. C., "Emission spectra and etching of polymers and graphite irradiated by excimer lasers," J. Appl. Phys. **56** (7), 2120-2126, 1984.

[18] Barnier, F. Dyer, P. E. Monk, P. Snelling, H. V. and Rourke, H., "Fiber optic jacket removal by pulsed laser ablation," J. Phys. D **33**, 757-759, 2000.

[19] Snelling, H. V., Walton, C. D., and Whitehead, D. J., "Polymer jacket stripping of optical fibers by laser irradiation," Appl. Phys. A **79** (4-6), 937-940, 2004.

[20] Smelser, C. W., Mihailov, S. J., and Grobnic, D., "Rouard's method modeling of type I-IR fiber Bragg gratings made using an ultrafast IR laser and a phase mask," J. Opt. Soc. Am. B **23** (10), 2011-2017, 2006.

[21] Baudach, S., Bonse, J., and Kautek, W., "Ablation experiments on polyimide with femtosecond laser pulses," Appl. Phys. A **69,** S395 - S398, 1999.

[22] Martin, S., Krüger, J., Hertwig, A., Fiedler, A., and Kautek, W., "Femtosecond laser interaction with protection materials," Appl. Surf. Sci. **208-209,** 333-339, 2003.

[23] Poladian, L., "Understanding profile-induced group-delay ripple in Bragg gratings," Appl. Opt. **39** (12), 1923-1926, 2000.

[24] Lemaire, P. J. "Reliability of optical fibers exposed to hydrogen: prediction of long-term loss increases," Opt. Eng. **30** (6), 780-789, 1991.

[25] Gower, M.C. ñLaser Processing in Manufacturingò, Chpt. 9, Crafer, R.C., and Oakley, P.J. eds., Chapman & Hall 1993.